Bioelectrochemistry 172 (2026) 109374

Contents lists available at ScienceDirect

Bioelectrochemistry

journal homepage: www.journals.elsevier.com/bioelectrochemistry

Reduced mediators released by cyanobacteria during exoelectrogenesis detected using differential pulse voltammetry☆

Laura T. Wey [a,*,1], Monica Brachi [b,1], Yagut Allahverdiyeva [a], Shelley D. Minteer [b,*]

[a] Department of Life Technologies, University of Turku, Finland
[b] Department of Chemistry, Missouri University of Science and Technology, USA

ARTICLE INFO

Keywords:
Exoelectrogenesis
Cyanobacteria
Photosynthesis
Differential pulse voltammetry
Mediators

ABSTRACT

Cyanobacteria generate electrical current through exoelectrogenesis (extracellular electron transfer) downstream of photosynthesis, yet the identity of the endogenous redox mediator(s) responsible remains unresolved. Here, we apply differential pulse voltammetry (DPV) to detect and characterise redox-active species released by *Synechocystis* sp. PCC 6803 under illumination. To enable sensitive detection, we developed an electrolyte intermediate between BG11 (Blue-Green-11) growth medium and MOPS (3-(N-morpholino)propanesulfonic acid) buffer that minimises background electrochemical interference while maintaining short-term cellular functionality. DPV revealed multiple light-enhanced oxidation peaks (0.1–0.65 V vs. saturated calomel electrode (SCE)) that were not resolvable using cyclic voltammetry, providing evidence that cyanobacteria release reduced compounds during exoelectrogenesis. These signals were partially reproduced in cell exudates and absent in controls, confirming their biological origin. The lack of corresponding reduction peaks suggests irreversible redox processes. Comparison with candidate mediators showed that NADPH and 4-hydroxybenzoate, an intermediate in plastoquinone biosynthesis, exhibit only partially similar electrochemical behaviour compared to cells and do not fully account for the measured responses. Collectively, our results indicate that exoelectrogenesis in *Synechocystis* sp. PCC 6803 involves a mixture of redox-active species rather than a single mediator. This study establishes DPV as a powerful tool for in situ detection of cyanobacterial mediators and provides new insights into the mechanisms of photosynthetic extracellular electron transfer.

1. Introduction

Photosynthetic microorganisms, including cyanobacteria and algae, can transfer electrons to their external environment in a process known as exoelectrogenesis or extracellular electron transfer [1]. In many systems, a substantial current is observed in the dark, with illumination leading to a further increase in current. The light-dependent component is attributed to electrons derived from oxygenic photosynthesis, where water oxidation at photosystem II (PSII) supplies electrons to the photosynthetic electron transport chain (PETC). The electrons are proposed to exit the PETC downstream of photosystem I (PSI). However, the exact point of exit from the PETC remains to be determined, whether it be PSI, ferredoxin or NADPH.

In the model cyanobacterium *Synechocystis* sp. PCC 6803 (hereafter *Synechocystis*), evidence suggests that electron export occurs through indirect extracellular electron transfer mechanisms involving soluble, diffusible redox mediator(s) released by the cells [1–3]. This interpretation is supported by several observations: stirring the electrolyte abolishes steady-state photocurrent [4], increasing cell envelope permeability by a gentle pressurized treatment [5] or by removing the outer membrane entirely [6] enhances current output, and structural modifications to the outer membrane [6] or peptidoglycan layer [7] alter photocurrent kinetics under dark to light transitions. Furthermore, in *Synechocystis* electron export does not occur via direct extracellular electron transfer mechanisms commonly found in heterotrophic electrogens. For example, there is no convincing electrochemical or genetic evidence for conductive microbial nanowires in the form of type IV pili [7,8], redox species embedded in the exopolysaccharide matrix [4], or multi-heme cytochrome systems facilitating direct electron transfer [9].

Experimental studies have suggested several properties of the

☆ This article is part of a Special issue entitled: 'Photobioelectrochemistry' published in Bioelectrochemistry.

* Corresponding authors.
E-mail addresses: laura.wey@utu.fi (L.T. Wey), shelley.minteer@mst.edu (S.D. Minteer).

[1] Contributed equally.

https://doi.org/10.1016/j.bioelechem.2026.109374
Received 30 March 2026; Received in revised form 17 June 2026; Accepted 2 July 2026
Available online 3 July 2026

endogenous redox mediator. Previous studies suggested that the mediator is small (on the order of a few kilodaltons), because redox peaks in cyclic voltammetry persisted when cell exudate in BG11 growth medium was then filtered [5,6]. In addition, the mediator is suggested to be temperature-sensitive, because the redox behaviour was inactivated after heat-treatment [5]. Further, it is proposed that the mediator is amphiphilic by crossing the cell boundary by diffusion across the plasma membrane (and outer membrane), although transport via a transmembrane protein has not been ruled out. Previous studies suggested that the mediator has reversible redox behaviour, as indicated by presence of oxidation and reduction peaks in cyclic voltammograms of cyanobacterial cells in BG11 electrolyte, and these studies suggest the mediator has a midpoint potential of +0.34 V vs. standard hydrogen electrode (SHE) [5,10]. However, interpretation of electrochemical signals in previous studies has been complicated by recent reports of contributions from components in BG11, including proton-coupled oxidation of manganese chloride [6,11]. The mediator has been both proposed [12] and refuted [6] to be NADPH. Despite this general framework, the identity of all the endogenous electron mediator(s) is uncertain. Moreover, it remains to be investigated whether a single or multiple redox species are responsible for the exoelectrogenesis in *Synechocystis,* and if the molecules are the same in the dark and light.

Insights from heterotrophic electroactive bacteria provide a useful framework for considering potential electron mediators in cyanobacteria. In organisms such as *Shewanella* spp., extracellular electron transfer is facilitated by secreted flavins (flavin mononucleotide and riboflavin) [13]. However, there is no genomic evidence of secretion of flavins in cyanobacteria [9]. In organisms such as *Pseudomonas aeruginosa*, extracellular electron transfer is facilitated by secreted phenazines (e.g. pyocyanin) [14]. However, phenazines are not naturally produced by cyanobacteria [9,15]. Multiple organisms use quinones [16], such as hydroquinone derivatives by *Escherichia coli* [17] and 1,4-dihydroxy-2-naphthoic acid (DHNA) by *Shewanella oneidensis* MR-1 [18]. Cyanobacteria possess quinone biosynthetic pathways, including phylloquinone (vitamin K_1), which serves as the primary electron acceptor in photosystem I and is synthesised via intermediates including DHNA [19]. In addition, benzoquinones such as plastoquinone (PQ) play central roles in photosynthetic and respiratory electron transport, suggesting that quinone-related compounds could plausibly act as endogenous mediators in exoelectrogenesis in cyanobacteria.

Thus far, attempts to identify the endogenous mediator in *Synechocystis* have primarily relied on techniques such as chronoamperometry [4,20], cyclic voltammetry [5,10], and fluorescence spectroscopy [6,12]. While these approaches have provided useful insights into exoelectrogenesis mechanisms, they are often limited by overlapping signals and interference from background electroactive species. Consequently, the detection and identification of low-abundance endogenous redox mediators remain challenging.

More advanced voltammetric techniques [21], including square wave voltammetry and differential pulse voltammetry (DPV), can be superior analytical tools compared to conventional cyclic voltammetry for detecting target analytes or unknown electroactive species. In DPV, small potential pulses (typically 20–50 mV) are superimposed onto a linear potential sweep, and the current difference before and after each pulse is measured. This approach suppresses capacitive background currents while enhancing faradaic signals, resulting in improved peak resolution. As such, DPV is particularly well-suited for the in situ detection of low-concentration or transient electroactive species.

The utility of DPV for investigating extracellular redox mediators has been demonstrated in studies of heterotrophic electrogens [21,22]. For example, DPV has been used to detect and identify flavins as redox species released by *Shewanella oneidensis* biofilms [13]. More broadly, DPV has become widely employed in electrochemical biosensing because of its rapid acquisition times and enhanced discrimination of Faradaic currents from background capacitive currents, which determine high sensitivity, selectivity and low limits of detection. Consequently, DPV-based biosensors have been developed for the sensitive detection and quantification of a wide range of analytes, including biologically derived metabolites such as neuropeptides, hormones and antioxidants [23,24], microbial pathogens [25], and environmental contaminants, which include photosynthesis-inhibiting herbicides [26].

In this study, we employed DPV to identify the endogenous electron mediator(s) released by *Synechocystis* cyanobacteria under illumination. We hypothesised that there could be multiple species and explored NADPH and a short-tail quinone in the PQ biosynthesis pathway as putative candidates.

2. Materials and methods

2.1. Strains and culture conditions

A glucose tolerant and non-motile strain of *Synechocystis* sp. PCC 6803 that originated from Aaron Kaplan's lab at The Hebrew University of Jerusalem, Israel, and was obtained from the University of Turku, Finland was used (genome: National Center for Biotechnology Information BioProject accession PRJNA1277488, Sample accession number SAMN49110441). Cultures were grown in BG11 medium buffered with 20 mM HEPES to pH 7.5 [27]. Culturing conditions were 30 °C, ambient air levels of CO_2, and 120 rpm shaking in a growth chamber (Solaris 4000, Thermo Scientific™, Waltham, MA, USA) with continuous 50 μmol photons m^{-2} s^{-1} of light provided by a light-emitting diode (LED) full spectrum grow lamp above (SF1000D, Spider Farmer, Shenzhen, China). Growth was monitored by measuring attenuance at 750 nm (OD750) using a Thermo Scientific Evolution 260 Bio ultraviolet-visible (UV–Vis) spectrophotometer (Thermo Scientific™, Waltham, MA, USA), and cultures were started at OD750 0.1. The chlorophyll *a* concentration was determined spectrophotometrically after extraction in methanol at 65 °C for 10 min. Samples were clarified by centrifugation (13,000*g*, 2 min, 21 °C), and concentrations were calculated using an extinction coefficient of 79.95 (Chl *a* mg)$^{-1}$ mL cm^{-1} [28].

2.2. Materials and chemicals

Carbon paper (AvCarb® MGL 190, Fuel Cell Store, Bryan, TX, USA) was used for the fabrication of working electrodes. Photosystem II activity was inhibited using 3-(3,4-dichlorophenyl)-1,1-dimethylurea (DCMU) (Millipore Sigma, Burlington, MA, USA). Candidate redox mediators tested were NADPH (Research Products International, Mt. Prospect, IL, USA) and sodium 4-hydroxybenzoate (H3766, Merck, Darmstadt, Germany).

2.3. Construction of bioanode

Carbon paper electrodes were cut into 1 × 3 cm pieces, and 1 × 2 cm area was covered with wax, leaving a geometric surface area of 1 cm^2. As the electrodes were not chemically or structurally modified, current densities reported throughout the study were calculated using this geometric surface area. Cells from 90 mL of cultures with an OD750 0.6–0.9 were harvested by centrifugation at 2300*g* for 20 min at 21 °C. Supernatant from this step was the BG11 exudate. The BG-MOPS exudate was formed by resuspending the cells in 10 mL BG-MOPS. Alternatively, cells were resuspended to a final concentration of 1 mg/mL (chlorophyll *a* 750–1250 μg/mL) in the solution used as electrolyte for that experiment (either fresh BG11 medium or BG-MOPS, Supplementary Table 1). To prepare an autoclaved cell sample, culture flasks were heated to 121 °C for 15 min before preparing to 1 mg/mL. 100 μL of 1 mg/mL cell mixture (chlorophyll 750–1250 μg/mL) was drop cast onto the electrode and held under stream of N_2 in a desiccator for 30 min–1 h until almost dry. A flow chart of the preparation of different biological samples for photoelectrochemical analysis is in Supplementary Fig. 12.

2.4. Photoelectrochemistry

Photoelectrochemical performance was measured using a three-electrode configuration with a Squidstat™ Prime potentiostat (Admiral Instruments, Tempe, AZ, USA). The setup comprised a carbon paper working electrode, saturated calomel electrode (SCE) (saturated KCl) reference electrode, and a platinum mesh counter electrode. Measurements were conducted in a standard glass three-electrode electrochemical cell. Electrolyte was 10 mL BG11 growth medium or BG11-like MOPS buffer (BG-MOPS, Supplementary Table 1) as specified. The electrochemistry parameters of cyclic voltammetry (CV), differential pulse voltammetry (DPV) and chronoamperometry experiments are described in each figure caption. CV and DPV experiments were always initiated by scanning with the forward direction. All potentials in this article are reported as V vs. SCE (saturated KCl). The light used in photoelectrochemistry experiments was a "cool" 3100 K white Fiber-Lite® Fiber Optic Illuminator (Model 190, Dolan-Jenner Industries, Boxborough, MA, USA), positioned at a distance to provide a light spot diameter able to just cover the working electrode with an of intensity 500 μmol photons m^{-2} s^{-1}. From chronoamperometry under light/dark cycles, the photocurrent was calculated as the difference in current during the last 5 s of the light period, baselined against the current during the dark period before the light period.

2.5. Biocompatibility assessment through photosynthesis and cell growth

Biocompatibility of BG-MOPS electrolyte was tested by measuring the photosynthetic activity and cell growth compared to BG11. Cells were harvested from BG11-grown culture and resuspended to a final chlorophyll concentration of 10 μg/mL. The cells were incubated for 2 h under culture conditions after which the photosynthetic activity was measured. The photosynthetic yield of photosystem II (Y(II)), was determined by measuring room temperature chlorophyll fluorescence of the cells in the electrolytes after 10 min dark adaptation using a pulse-amplitude modulation fluorimeter DUAL-PAM-100 (Heinz Walz GmbH, Effeltrich, Germany). The cells were illuminated with a red light-saturating pulse (5000 μmol photons m^{-2} s^{-1}, 500 ms) to measure maximum fluorescence. The cell growth was measured in liquid culture. Cells were harvested from the BG11-grown starting culture and resuspended in fresh BG11 or BG-MOPS OD750 = 0.1 and incubated under culture conditions. Growth after 3 days was measured by OD750 and photographs were taken of the flasks.

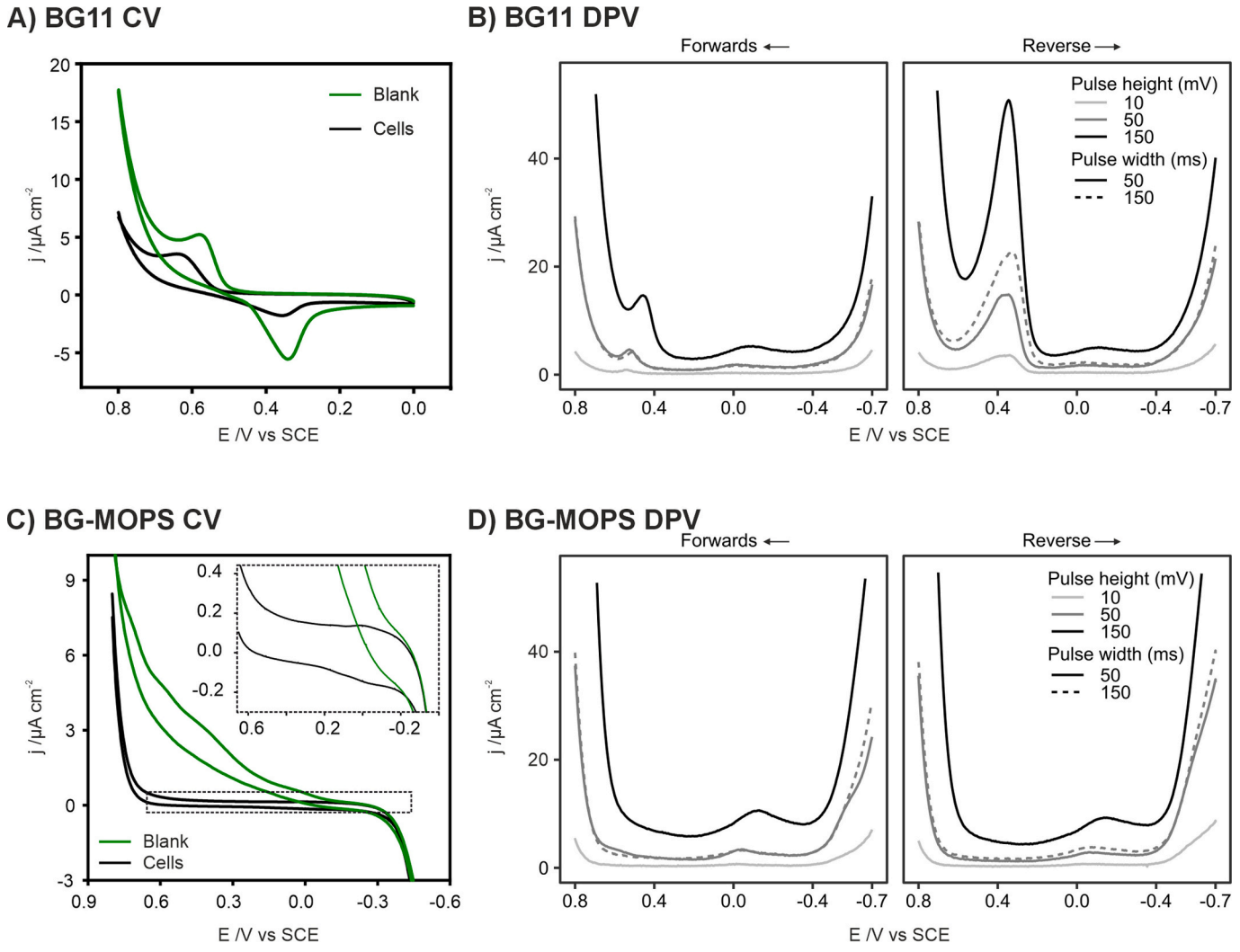

Fig. 1. Electrochemistry of different cyanobacteria-compatible electrolytes.
(A, C) Cyclic voltammograms. Scan rate 5 mV s^{-1}, carbon paper electrode, no loading (black) or cyanobacteria cells loaded (green), constant white light at 500 μmol photons m^{-2} s^{-1} intensity. (B, D) Differential pulse voltammograms. Potential step 5 mV, pulse height 10–150 mV, pulse width 50–150 ms, pulse period 200 ms, carbon paper electrode, no cyanobacteria cells loaded, darkness. (A, B) BG11 growth medium as electrolyte (BG11). (C, D) BG11-like MOPS buffer (BG-MOPS, Supplementary Table 1) as electrolyte. Data presented as one representative sample. Additional differential pulse voltammograms recorded at fixed electrochemical parameters are presented in Supplementary Fig. 1 as mean of replicates with shaded ribbons representing the standard error of the mean (SEM).

3. Results

3.1. BG11-like MOPS electrolyte prevents occlusion of redox mediators released by cyanobacteria during exoelectrogenesis

To establish a system to use advanced differential pulse voltammetry to detect redox mediators released by cyanobacteria during exoelectrogenesis, we first tested different electrolytes with carbon paper electrodes starting with simpler cyclic voltammetry (CV). The cyclic voltammogram of blank carbon paper electrodes in BG11 growth medium as the electrolyte showed an oxidation peak at +0.35 V vs. SCE and a reduction peak at +0.63 V vs. SCE (Fig. 1A – black). When cyanobacteria cells that had been grown in BG11 were loaded on carbon paper electrodes and scanned in BG11 electrolyte under illumination, the cyclic voltammogram was largely similar to that of the blank electrodes with an oxidation peak at +0.34 V vs. SCE and a reduction peak at +0.57 V vs. SCE (Fig. 1A – green). The slight shift observed, especially in the reduction peak between the two electrolytes, is likely due to the alteration of electron transfer kinetics and local pH changes in the presence of the cell film on the electrode surface. Next, we conducted more sensitive differential pulse voltammetry (DPV). The same oxidation and reduction peaks observed during CV measurements on the blank electrodes in BG11 electrolyte were visible in DPV measurements at different scanning parameters in the forward and reverse direction, respectively (Fig. 1B). Despite the elimination of capacitive currents by DPV, the presence of these prominent redox peaks, both in the absence and presence of cells and linked to the presence of trace minerals in BG11 growth media [27] suggests that this electrolyte is not suitable for the detection of redox mediators released by cyanobacteria during exoelectrogenesis due to the possible overlapping of signals in a similar potential range.

We therefore created a BG11-like MOPS buffer (hereafter called BG-MOPS, Supplementary Table 1) that has no redox active trace metals normally present in BG11 and maintains a buffered pH of 7.5 not using HEPES but using MOPS. MOPS is often preferred over HEPES buffer for microbial redox-sensitive electrochemical studies because of its lower complexation ability and interference with reactive intermediates, and it has been already validated as a good buffering system in phenazine-mediated systems [29]. The BG-MOPS contained sodium nitrate, phosphate, and carbonate at the same concentrations as in BG11 to preserve nutrient availability. The cyclic voltammogram of blank carbon paper electrodes in BG-MOPS electrolyte did not exhibit clear redox peaks (Fig. 1C – black). When cyanobacteria cells that had been grown in BG11 were loaded on the carbon paper electrode and scanned in BG-MOPS electrolyte under illumination, the cyclic voltammograms were different than those of blank electrodes above 0 V vs. SCE suggesting that BG-MOPS was a more suitable electrolyte (Fig. 1C – green). However, there were still no discernible redox peaks in the cell-loaded electrodes, which confirmed that CV is not an ideal technique for the detection of endogenously produced mediators.

Following the more promising approach of DPV, we conducted DPV initially by varying different electrochemical parameters (pulse height and pulse width) using blank carbon paper electrodes in BG-MOPS electrolyte. Only an oxidation peak and reduction peak at +0.1 V vs. SCE were observed (Fig. 1D), which were also present in the BG11 electrolyte voltammograms (Fig. 1B) and were assigned to the carbon paper electrodes. The presence of these peaks in pristine carbon materials is documented in the literature and commonly attributed to surface oxygen-containing functional groups [30,31]. To achieve a balance between measurement throughput and low background current, we chose 50 mV pulse height and 50 ms pulse width for subsequent measurements with cyanobacterial cells and BG-MOPS electrolyte.

To test the effect of the BG-MOPS on the exoelectrogenic performance of the cells, we performed chronoamperometry (CA) of BG11-grown cells in BG-MOPS electrolyte. When light was turned on during CA, the current evolving from the cyanobacteria cells increased, with characteristic kinetics as in BG11 electrolyte in previous studies (Fig. 2A, Supplementary Fig. 2) [7]. The photocurrent (difference between the steady state current in the light and dark) yielded from the cyanobacteria cells in BG-MOPS electrolyte was approximately 1.75 μA cm^{-2}, whereas there was negligible photocurrent from blank electrodes in BG-MOPS electrolyte. Additional negative controls of autoclaved cells and cells treated with DCMU inhibitor of photosystem II yielded significantly less photocurrent than cells.

To test the effect of the BG-MOPS on the photosynthetic performance of the cells, BG11-grown cells were transferred to BG-MOPS or fresh BG11 and after 2 h the change in the photosynthetic yield of photosystem II in a dark-adapted state, Y(II), was measured. The cyanobacterial cells in the BG-MOPS exhibited Y(II) values (0.26 ± 0.02) similar to cells in BG11 (0.280 ± 0.001, $P = 0.1136$, $n = 3$) (Supplementary Fig. 3A). We also measured the UV–Vis spectra of cells and observed no significant difference between peaks corresponding to chlorophyll *a* in the photosystems or phycobilin proteins in the phycobilisome light harvesting antennae (Supplementary Fig. 3B). These results indicate that the BG-MOPS electrolyte maintains the photosynthetic activity of the cyanobacterial cells for 2 h. However, when we tried to grow the cells in BG-MOPS they did not grow after 3 days (Supplementary Fig. 3C). These results indicate that BG-MOPS is suitable as a biocompatible electrolyte for short-term photoelectrochemical measurements of cells grown in BG11 for 2 h.

3.2. Cyanobacteria release reduced mediator(s) during exoelectrogenesis under illumination with multiple oxidation peaks

To capture the redox signatures of redox mediator(s) released by cyanobacteria during exoelectrogenesis, we loaded cyanobacteria on carbon paper electrodes and measured DPV in BG-MOPS electrolyte. In the dark, two small oxidation peaks were visible at 0.65 V and 0.55 V vs. SCE superimposed on an elevated current >0.4 V vs. SCE in the forward scanning direction (Fig. 3A – black), differently from blank electrodes (Fig. 3B). After 1 h of illumination, these peaks appeared more pronounced with a concomitant increase in current in the 0–0.4 V vs. SCE window (Fig. 3A – yellow). When the scans from light and dark treatments were subtracted and baseline corrected, the oxidation peaks at 0.65 V and 0.55 V vs. SCE appeared well resolved and an additional oxidation peak at 0.3 V vs. SCE was revealed (Fig. 3– green and insert). The peak at 0 V vs. SCE was consistent with the signal from the carbon paper electrodes (Fig. 1B–D), and in some biological replicates there was an additional peak around 0.1 V vs. SCE (Supplementary Fig. 4A). Oxidation peaks >0.1 V vs. SCE were absent in blank carbon paper electrodes or when autoclaved cells were loaded (Fig. 3B,C). When cells were treated with the PSII-inhibitor DCMU no peaks >0 V vs. SCE were visible (Fig. 3D), and DCMU itself at higher concentrations was characterized by an oxidation peak around 0.3 V vs. SCE, and an enhanced peak around at 0 V vs. SCE likely attributable to the untreated carbon paper (Supplementary Fig. 5). From cells there were no clear reduction peaks in the reverse scanning direction, although the current was higher in the light treated sample than the dark (Fig. 3A), whereas the negative control samples had the same background current in light and dark in the reverse scanning direction (Supplementary Fig. 6).

To confirm the reduced species identified in DPV measurements of cyanobacteria on electrodes (Fig. 3A) are released from the cells, we incubated cells in BG-MOPS for 15 min and then analysed the electrochemistry of the BG-MOPS exudate. The cyclic voltammogram of bare carbon paper electrodes in the BG-MOPS exudate appeared different from the cyclic voltammogram in plain BG-MOPS electrolyte showing an oxidation peak at 0.4 V vs. SCE (Fig. 4A), significantly more pronounced than the one obtained with cells in BG-MOPS (Fig. 1C).

The differential pulse voltammogram of bare carbon paper electrode in the BG-MOPS exudate showed a clear oxidation peak at 0.25 V vs. SCE and a small oxidation peak at 0.65 V vs. SCE in the forwards direction scan (Fig. 4B, Supplementary Fig. 7). The oxidation peak at 0.65 V vs.

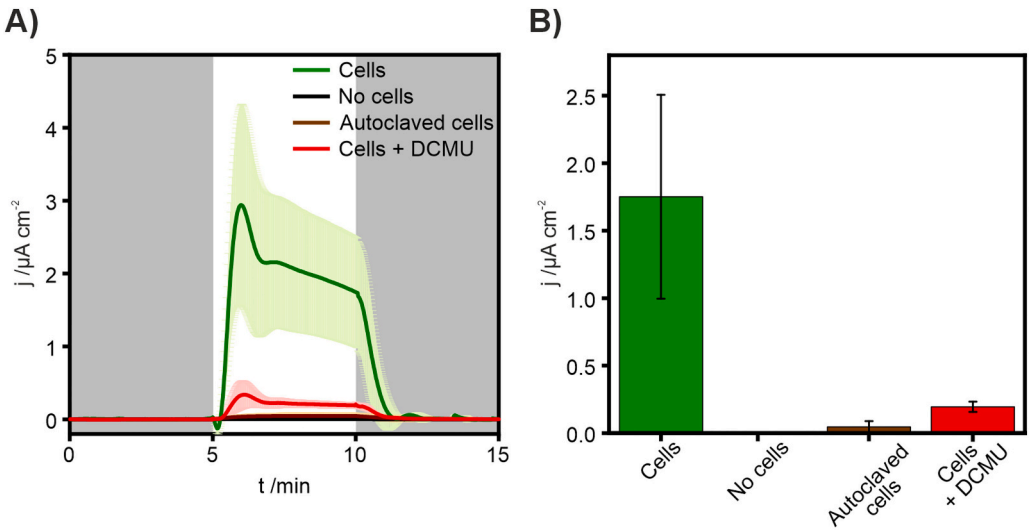

Fig. 2. Photocurrent output of cyanobacteria in BG-MOPS.
(A) Photocurrent kinetics. (B) Photocurrent magnitude. Applied potential 0.5 V vs. SCE, sampling 1 s^{-1}, carbon paper electrodes, white light at 500 µmol photons m^{-2} s^{-1} intensity. Data presented as mean, the shaded ribbons in panel A and error bars in panel B represent SEM, $n = 3$. Data presented with different y-axes to more clearly see the kinetics in Supplementary Fig. 2.

SCE was more pronounced after baseline correction (Fig. 4B – insert). Additional oxidation peaks at 0.55 V or around 0.1 V vs. SCE were not observed from the BG-MOPS exudate. There were no reduction peaks in the reverse scanning direction >0 V vs. SCE. UV Vis spectra of the BG-MOPS exudate had three absorbance peaks at 330, 440 and 480 nm together giving the BG-MOPS exudate a yellow colour (Fig. 4C).

The exudate from cells grown in BG11 was also collected and analysed. As with cells (Fig. 1A), the cyclic voltammogram of carbon paper in BG11 exudate and plain BG11 electrolyte were similar (Supplementary Fig. 8A), with a similar shift in peak potential to that observed previously between cells loaded on electrodes versus bare electrodes in BG11. These findings further demonstrate that BG11 is not a suitable electrolyte for detecting the redox mediator(s) released by cyanobacteria during exoelectrogenesis. Similarly, DPV with different electrochemical parameters on blank carbon paper electrode in BG11 exudate only showed an oxidation peak at 0.5 V vs. SCE in the forward scanning direction (Supplementary Fig. 8B,C). UV Vis spectra of the BG11 exudate had three absorbance peaks at 320, 360 and 400 nm (Supplementary Fig. 8D).

These results indicate that cyanobacteria release reduced mediator (s) during the exoelectrogenesis mechanism under illumination with multiple oxidation peaks. These signals originate from live cells performing photosynthesis, rather than cell-surface redox proteins. The oxidation of these reduced mediators is irreversible, as no redox peaks were detected in the reverse scans.

3.3. NADPH and a plastoquinone biosynthesis intermediate exhibit some similarity to cyanobacteria redox signatures

To identify the redox species released from cyanobacterial cells (Fig. 3A, Fig. 4B), we shortlisted two candidate mediators for comparison. NADPH was initially considered due to its central role as the primary electron carrier generated downstream of photosystem I (Fig. 5A) [1], as well as a previous report that it functions as an endogenous mediator in *Synechocystis* [12]. Based on analysis of *Synechocystis* metabolic pathways, we also identified 4-hydroxybenzoate as a second candidate, as it is a precursor in plastoquinone-9 biosynthesis (Fig. 5B). Plastoquinone-9 is synthesised from chorismate via 4-hydroxybenzoate, which is subsequently modified by the addition of an isoprenoid tail. In cyanobacteria, the plastoquinone (PQ) pool consists of lipid-soluble, mobile electron carriers: plastoquinone (PQ) and plastoquinol (PQH_2). The PQ pool links the photosynthetic and respiratory electron transport chains within the thylakoid membrane, while an additional plastoquinone pool is present in the cytoplasmic membrane [1].

Cyclic voltammetry of the individual candidate molecules in BG-MOPS electrolyte showed distinct redox behaviour for both NADPH and 4-hydroxybenzoate (Supplementary Fig. 9). To enable direct comparison with cyanobacterial signals, we next performed DPV of each candidate under the same electrochemical conditions. NADPH exhibited an oxidation peak at 0.55 V vs. SCE (Fig. 5C). On the other hand, 4-hydroxybenzoate exhibited oxidation peaks at 0.7 and 0.3 V vs. SCE, in addition to a peak around 0 V vs. SCE that overlaps with the signal from carbon paper (Fig. 5D). NADPH and 4-hydroxybenzoate exhibited quasi-reversible redox behaviour with reduction peaks appearing predominantly in the forward and reverse scanning directions, respectively (Fig. 5C,D). When NADPH and 4-hydroxybenzoate were combined in a 10:1 ratio, the resulting DPV profile showed oxidation peaks at 0.55 and 0.3 V vs. SCE, in addition to a peak around 0 V vs. SCE that overlaps with the signal from carbon paper (Fig. 5E).

UV–Vis spectroscopy in both BG11 and BG-MOPS demonstrated that NADPH exhibited absorbance peaks at 260 and 340 nm (Supplementary Fig. 10A), while 4-hydroxybenzoate showed a single peak at 260 nm (Supplementary Fig. 10B). These spectral features differ from those observed in cyanobacterial exudates (Fig. 4C).

To briefly assess their functional roles, we performed chronoamperometry experiments. In the absence of cells, NADPH was able to contribute to pseudo-photocurrent generation at an applied potential of 0.5 V vs. SCE, but not at 0.1 V vs. SCE (Supplementary Fig. 10A). In contrast, 4-hydroxybenzoate did not contribute to pseudo-photocurrent generation at either applied potential tested (Supplementary Fig. 10B). Sequential additions of 4-hydroxybenzoate to cyanobacterial cells did not enhance photocurrent at an applied potential of 0.5 V vs. SCE (Supplementary Fig. 11C) suggesting that 4-hydroxybenzoate does not act as an exogenous electron mediator under these conditions.

4. Discussion

4.1. Evidence for multiple mediator species

DPV measurements revealed multiple oxidation peaks (0.65, 0.55, 0.3, 0.1 V vs. SCE) under illumination and without cell death (autoclaving) or photosynthesis inhibition (DCMU treatment), providing

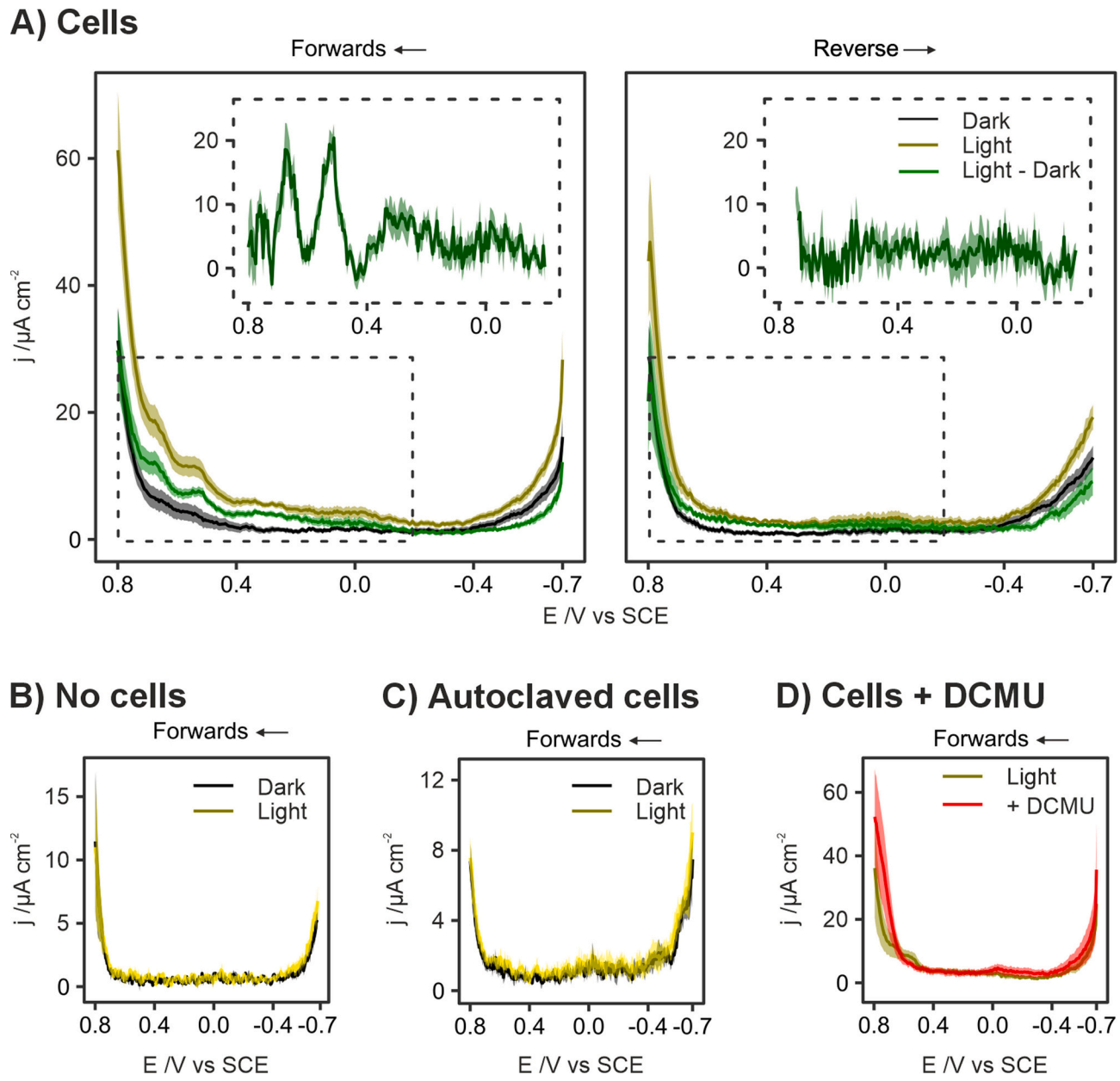

Fig. 3. Redox signatures of cyanobacteria on electrodes, and negative controls.
(A) Cells. (B) No cells. (C) Autoclaved cells. (D) Cells treated with photosynthesis inhibitor DCMU (1 mM). Differential pulse voltammograms, potential step 5 mV, pulse height 50 mV, pulse width 50 ms, pulse period 200 ms, carbon paper electrode, BG-MOPS electrolyte. Darkness – black, 1 h treatment with white light at 500 µmol photons m^{-2} s^{-1} intensity – yellow, difference between light and dark – green. Data presented as mean, the shaded ribbons represent SEM, (A) $n = 5$–8 (from population 1, more replicates in Supplementary Fig. 6), (B, C) $n = 3$, (D) $n = 4$. Insert in (A) baseline corrected. (For interpretation of the references to colour in this figure legend, the reader is referred to the web version of this article.)

strong evidence that *Synechocystis* releases reduced redox-active compounds during photosynthetic activity. Most redox-active species exhibit one or two redox processes, and it is uncommon for a single species to display four distinct oxidation peaks.

The different oxidation peaks presented with different relative intensities in different biological samples, which we classified into at least three sub-populations (Supplementary Fig. 4). Furthermore, the electrochemical signatures observed from cell-loaded electrodes were only partially reproduced in the corresponding cell exudates. While peaks at ~0.3 V and ~0.65 V vs. SCE were detected in the exudate, others, most notably the ~0.55 V vs. SCE peak, were absent. The variety of peak combinations suggests that the mechanism of exoelectrogenesis in *Synechocystis* does not rely on a single mediator, but rather involves a mixture of redox-active compounds. This mechanism is consistent with heterotrophic electrogens such as *Shewanella* spp., where multiple endogenous mediators (e.g., flavins, quinones) contribute to extracellular electron transfer [13,18]. Similarly, voltammograms of biofilms of *Geobacter sulfurreducens* exhibit multiple and different oxidation peaks when grown under different applied potentials, suggesting the presence of several redox-active components involved in extracellular electron transfer depending on the metabolic state of the cells [32,33].

However, the discrepancy between cells and exudate signals could arise from other factors: (i) rapid turnover or instability of certain mediators outside the cell, (ii) adsorption or transformation at the electrode surface, or (iii) the requirement for continuous cellular metabolism to sustain specific redox species. It is also possible that some signals observed in cell-loaded electrodes arise from transient, surface-associated intermediates rather than freely diffusible mediators.

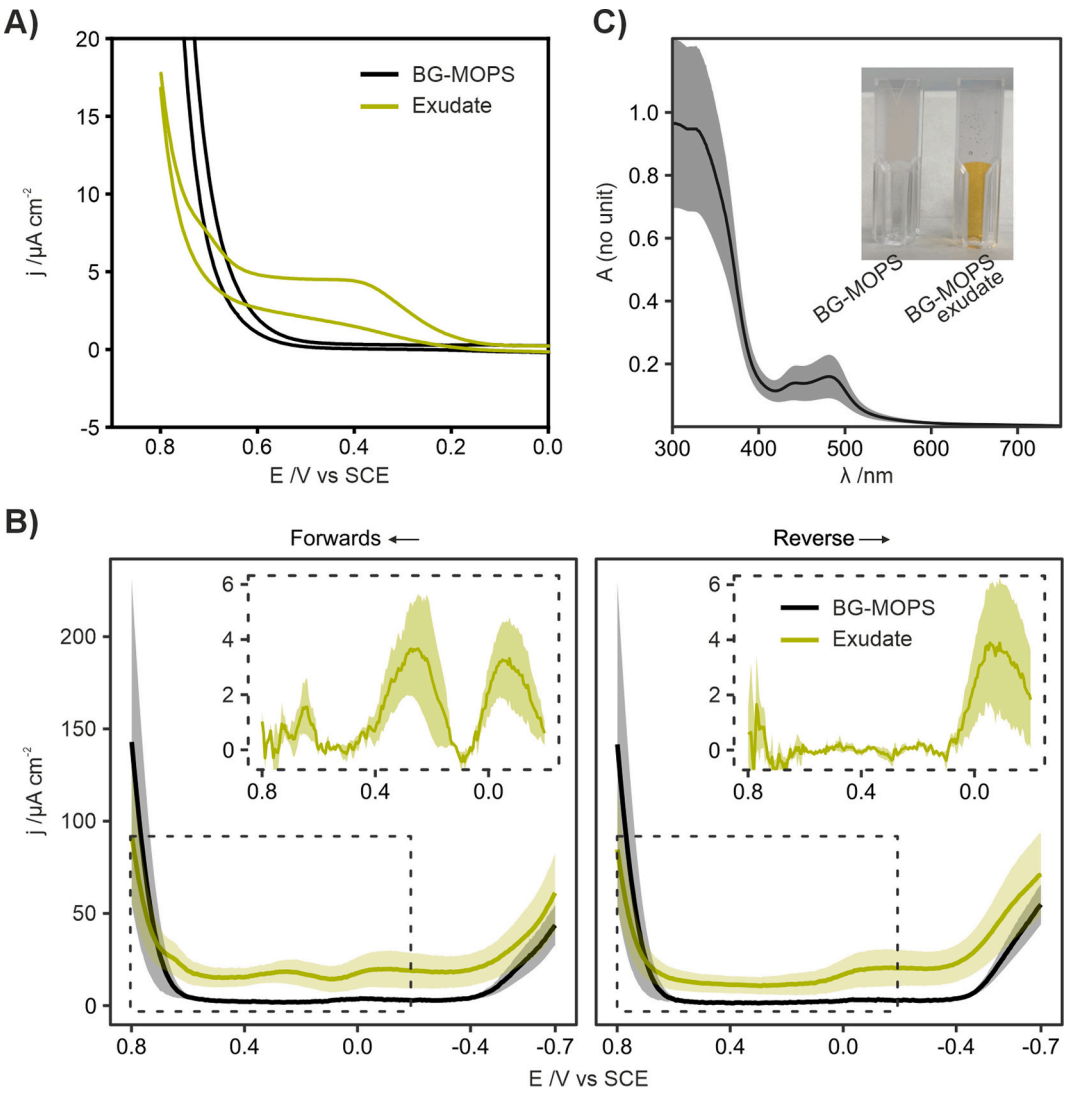

Fig. 4. Redox signatures of cell exudate in BG-MOPS.
(A) Cyclic voltammograms. Scan rate 5 mV s^{-1}. (B) Differential pulse voltammograms. Insert baseline corrected. Potential step 5 mV, pulse height 50 mV, pulse width 50 ms, pulse period 200 ms. (A, B) Carbon paper electrode, cell exudate in BG-MOPS, white light at 500 µmol photons m^{-2} s^{-1} intensity. (C) UV–Vis spectra of cell exudate in BG-MOPS. Data presented as (A) representative sample, (B–C) mean, the shaded ribbons SEM, (B) $n = 3$, (C) $n = 7$. More electrochemical parameters of (B) in Supplementary Fig. 7.

Consistent with this possibility, condition-dependent redox features have been observed in DPVs of *G. sulfurreducens* biofilms that were not directly associated with electrocatalytic activity [33].

4.2. Implications for identities of mediators

A key feature of the DPV data of photosynthesizing cells is the absence of corresponding reduction peaks in the reverse scans, indicating that the observed oxidation processes are largely irreversible under the experimental conditions.

NADPH has been proposed as the endogenous mediator in previous studies [12], and was therefore investigated here. Schlosberg et al. identified NADPH as the major redox mediator in cyanobacteria by its detection in the exudate and increase in the generated photocurrent upon exogenous addition [12]. However, Kusama et al. found no evidence of NADPH in cell supernatants by fluorescence mapping, enzymatic analysis, or LC-MS/MS analysis [6]. Further Wroe et al. discuss that the properties of NADPH do not match the electrochemical behaviour, notably reversibility and mid-point potential, of the mediator observed in CV by other authors [3,10].

NADPH is oxidized to $NADP^+$ via a two-electron, proton-coupled hydride transfer. It has a mid-point potential of around 0.55 V vs. SCE and its oxidation potential matches the one observed with cells. However, NADPH alone did not reproduce the full set of electrochemical features detected in cells. Furthermore, NADPH was also found to contribute to a pseudo-photocurrent at higher applied potentials (e.g., 0.5 V vs. SCE), complicating interpretation of contribution to photocurrent from lysed cells at these potentials.

In addition to NADPH, we explored 4-hydroxybenzoate, a precursor in plastoquinone biosynthesis. Compared to NADPH, this compound is less characterized. When tested in solution it displayed multiple peaks in the 0–0.4 V vs. SCE range similarly to cells. However, this candidate, similarly to NADPH, did not reproduce the full set of electrochemical features observed with cell-loaded electrodes, displaying reversible peaks with increased intensity in the reverse scan. Furthermore, 4-hydroxybenzoate was not able to enhance photocurrent when added exogenously.

The experiments conducted in the presence of both dissolved NADPH and 4-hydroxybenzoate in the BG-MOPS electrolyte, show varied electrochemical behaviour dependent on their relative ratio and order of

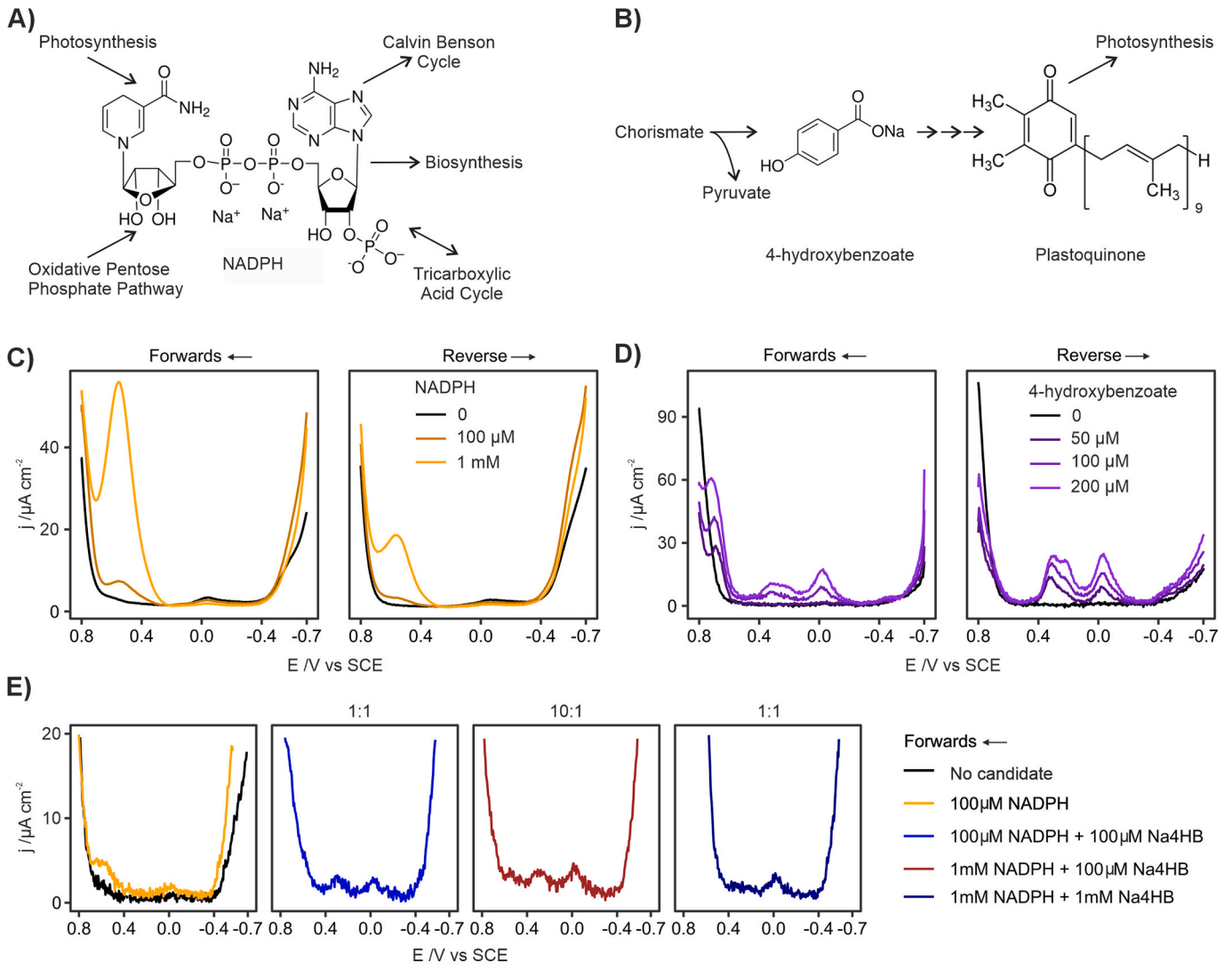

Fig. 5. Electrochemical performance of candidates molecules for the endogenous redox mediator(s) released by cyanobacteria during exoelectrogenesis. (A, B) Schematic showing the positions of candidates NADPH and 4-hydroxybenzoate (Na4HB) in cyanobacteria metabolism. (C, D) DPVs of individual candidates. (E) DPVs of candidates in sequential combinations. Potential step 5 mV, pulse height 50 mV, pulse width 50 ms, pulse period 200 ms, carbon paper electrode, BG-MOPS electrolyte. Data presented as representative sample.

addition (Fig. 5E). This suggests the occurrence of a chemical reaction involving the two mediators. The released compounds may undergo follow-up chemical reactions after oxidation, such as degradation, radical coupling, polymerisation, or reaction with dissolved oxygen, therefore complicating the analysis.

4.3. *Electrolyte design as a critical determinant of mediator detection*

A key outcome of this work is the demonstration that the commonly used BG11 growth medium is unsuitable for resolving mediator-derived electrochemical signals. Prominent redox peaks observed in both CV and DPV of BG11 electrolyte, even in the absence of cells, indicate that trace metal components obscure biologically derived signals within similar potential windows. This interference likely explains different conclusions in previous studies attempting to identify endogenous mediators using BG11 electrolyte and CV [5,10]. Previous studies predominantly investigating exoelectrogenesis using chronoamperometry measurements have already realised this, and modified the BG11 composition and pH to avoid pseudo-photocurrents [6,11].

By contrast, the development of the BG-MOPS electrolyte enabled a substantial improvement in signal clarity by removing redox-active trace metals, while maintaining essential nutrients and buffering capacity. In this system, background currents were minimised, allowing the emergence of distinct oxidation peaks attributable to cyanobacterial photosynthetic activity. These findings highlight the importance of carefully controlling electrolyte composition when probing biological redox processes.

However, this improved electrochemical resolution came with trade-offs. BG-MOPS did not support long-term cell growth. So even though photosynthetic activity was maintained short-term for DPV measurements, the absence of trace metals could still affect other natural mediator production or secretion pathways. In addition, differences in UV–Vis spectra between BG-MOPS and BG11 exudates suggest that electrolyte composition could also influence the stability or chemical reactivity of the released compounds, potentially through interactions such as metal complexation that alter their electronic and redox properties. Consequently, electrolyte-dependent behaviour complicates mediator identification and may contribute to discrepancies reported in the evolving literature [2,3], underscoring the need for careful control and reporting of experimental conditions and for approaches that balance electrochemical transparency with physiological relevance.

5. Conclusions and future directions

In this study we demonstrated that differential pulse voltammetry (DPV) enables the detection of reduced mediator(s) released by *Synechocystis* cyanobacteria during exoelectrogenesis under illumination, revealing multiple oxidation peaks that are not resolvable using conventional cyclic voltammetry (CV). Central to this advance was also the development of a BG11-like MOPS buffer (BG-MOPS), which minimises electrochemical background interference from conventional BG11 while maintaining cellular functionality during photoelectrochemical measurements. Our results provide electrochemical evidence that cyanobacteria release reduced compound(s) during exoelectrogenesis in an indirect electron transfer mechanism, rather than relying on direct electron transfer mechanisms such as membrane-associated redox proteins. The irreversible behaviour and partial reproducibility of these signals in cell exudates further suggest that a mixture of reduced compounds is involved, rather than a single mediator. Although the exact identity of the mediator(s) remains unresolved, the partial similarity of the observed signals to NADPH and short-chain quinones highlights promising targets for future investigation.

Despite the effectiveness of DPV in resolving mediator-derived signals, several limitations and opportunities for further development remain. The need for baselining DPV measurements to reveal sharper peaks, especially at 0.3 V vs. SCE, suggests that mediator flux or electrode–cell interactions may be suboptimal. These could possibly be improved through electrode surface functionalisation [34], optimisation of cell loading, or further modification of electrolyte composition.

More fundamentally, the interpretation of DPV signals remains indirect. Definitive identification of the mediator(s) will require complementary analytical techniques, such as chromatography, mass spectrometry, or spectroelectrochemical methods. In addition, integrating electrochemical measurements with systems biology approaches, including proteomics and metabolomics, in our ongoing research may also help link specific redox signatures to proteins or metabolites.

Finally, it remains unclear whether the mediator profile observed in *Synechocystis* is conserved across other cyanobacterial species or photosynthetic microorganisms, or whether it varies with environmental conditions, such as light intensity, trophic mode, nutrient availability, or salinity. Addressing these questions will be essential for developing a comprehensive understanding of photosynthetic exoelectrogenesis and for advancing the design of bioelectrochemical systems based on cyanobacteria.

CRediT authorship contribution statement

Laura T. Wey: Writing – review & editing, Writing – original draft, Visualization, Project administration, Investigation, Funding acquisition, Formal analysis, Data curation, Conceptualization. **Monica Brachi:** Writing – review & editing, Writing – original draft, Visualization, Methodology, Investigation, Formal analysis, Data curation, Conceptualization. **Yagut Allahverdiyeva:** Project administration, Funding acquisition. **Shelley D. Minteer:** Writing – review & editing, Project administration, Conceptualization.

Declaration of competing interest

The authors declare the following financial interests/personal relationships which may be considered as potential competing interests: Laura Wey reports financial support was provided by Novo Nordisk Foundation. Laura Wey reports financial support was provided by Research Council of Finland. Yagut Allahverdiyeva reports financial support was provided by Research Council of Finland. If there are other authors, they declare that they have no known competing financial interests or personal relationships that could have appeared to influence the work reported in this paper.

Acknowledgements

Ella Andersin and Arun FNU are acknowledged for assistance with cell culture. Pia Damlin and Pulmu Eloranta are acknowledged for discussion about functionalisation of electrode surfaces. This work was supported by the Novo Nordisk Foundation (grant number NNF22OC0079717), Research Council of Finland (grant numbers 355335, 368729), and Kummer Institute Center for Resource Sustainability.

Appendix A. Supplementary data

Supplementary data to this article can be found online at https://doi.org/10.1016/j.bioelechem.2026.109374.

Data availability

Data is available at Zenodo repository, at DOI: 10.5281/zenodo.21189102.

References

[1] L.T. Wey, P.B. Bos, M. Crosbie, P. Ortega Martínez, A. Tiwari, L. Nikkanen, Electron transport reactions of cyanobacterial photosynthesis and state-of-the-art in vivo measurement techniques, Plant Physiol. (2026) kiag107, https://doi.org/10.1093/plphys/kiag107.
[2] H. Zhu, H. Wang, Y. Zhang, Y. Li, Biophotovoltaics: recent advances and perspectives, Biotechnol. Adv. 64 (2023) 108101, https://doi.org/10.1016/j.biotechadv.2023.108101.
[3] E.I. Wroe, R.M. Egan, S.J. Willyam, L. Shang, J.Z. Zhang, Harvesting photocurrents from cyanobacteria and algae, Curr. Opin. Electrochem. 46 (2024) 101535, https://doi.org/10.1016/j.coelec.2024.101535.
[4] L.T. Wey, E.I. Wroe, V. Sadilek, L. Shang, X. Chen, J.Z. Zhang, C.J. Howe, Fourfold increase in photocurrent generation of *Synechocystis* sp. PCC 6803 by exopolysaccharide deprivation, Electrochim. Acta 497 (2024) 144555, https://doi.org/10.1016/j.electacta.2024.144555.
[5] G. Saper, D. Kallmann, F. Conzuelo, F. Zhao, T.N. Tóth, V. Liveanu, S. Meir, J. Szymanski, A. Aharoni, W. Schuhmann, A. Rothschild, G. Schuster, N. Adir, Live cyanobacteria produce photocurrent and hydrogen using both the respiratory and photosynthetic systems, Nat. Commun. 9 (2018) 2168, https://doi.org/10.1038/s41467-018-04613-x.
[6] S. Kusama, S. Kojima, K. Kimura, G. Shimakawa, C. Miyake, K. Tanaka, Y. Okumura, S. Nakanishi, Order-of-magnitude enhancement in photocurrent generation of *Synechocystis* sp. PCC 6803 by outer membrane deprivation, Nat. Commun. 13 (2022) 3067, https://doi.org/10.1038/s41467-022-30764-z.
[7] L.T. Wey, J.M. Lawrence, X. Chen, R. Clark, D.J. Lea-Smith, J.Z. Zhang, C.J. Howe, A biophotoelectrochemical approach to unravelling the role of cyanobacterial cell structures in exoelectrogenesis, Electrochim. Acta 395 (2021) 139214.
[8] M.A. Thirumurthy, A. Hitchcock, A. Cereda, J. Liu, M.S. Chavez, B.L. Doss, R. Ros, M.Y. El-Naggar, J.T. Heap, T.S. Bibby, A.K. Jones, Type IV pili-independent photocurrent production by the cyanobacterium *Synechocystis* sp. PCC 6803, Front. Microbiol. 11 (2020) 1344, https://doi.org/10.3389/fmicb.2020.01344.
[9] A.J. McCormick, P. Bombelli, R.W. Bradley, R. Thorne, T. Wenzel, C.J. Howe, Biophotovoltaics: oxygenic photosynthetic organisms in the world of bioelectrochemical systems, Energy Environ. Sci. 8 (2015) 1092–1109, https://doi.org/10.1039/c4ee03875d.
[10] J.Z. Zhang, P. Bombelli, K.P. Sokol, A. Fantuzzi, A.W. Rutherford, C.J. Howe, E. Reisner, Photoelectrochemistry of photosystem II in vitro vs in vivo, J. Am. Chem. Soc. 140 (2018) 6–9, https://doi.org/10.1021/jacs.7b08563.
[11] B. Lai, H. Schneider, J. Tschörtner, A. Schmid, J.O. Krömer, Technical-scale biophotovoltaics for long-term photo-current generation from Synechocystis sp. PCC6803, Biotechnol. Bioeng. 118 (2021) 2637–2648, https://doi.org/10.1002/bit.27784.
[12] Y. Shlosberg, B. Eichenbaum, T.N. Tóth, G. Levin, V. Liveanu, G. Schuster, N. Adir, NADPH performs mediated electron transfer in cyanobacterial-driven bio-photoelectrochemical cells, iScience 24 (2021) 101892, https://doi.org/10.1016/J.ISCI.2020.101892.
[13] E. Marsili, D.B. Baron, I.D. Shikhare, D. Coursolle, J.A. Gralnick, D.R. Bond, Shewanella secretes flavins that mediate extracellular electron transfer, Proc. Natl. Acad. Sci. 105 (2008) 3968–3973, https://doi.org/10.1073/pnas.0710525105.
[14] L.S. Pierson, E.A. Pierson, Metabolism and function of phenazines in bacteria: impacts on the behavior of bacteria in the environment and biotechnological processes, Appl. Microbiol. Biotechnol. 86 (2010) 1659–1670, https://doi.org/10.1007/s00253-010-2509-3.
[15] E.R. Clifford, R.W. Bradley, L.T. Wey, J.M. Lawrence, X. Chen, C.J. Howe, J. Z. Zhang, Phenazines as model low-midpoint potential electron shuttles for photosynthetic bioelectrochemical systems, Chem. Sci. 12 (2021) 3328–3338, https://doi.org/10.1039/d0sc05655c.

[16] D.K. Newman, R. Kolter, A role for excreted quinones in extracellular electron transfer, Nature 405 (2000) 94–97, https://doi.org/10.1038/35011098.
[17] Y. Qiao, C.M. Li, S.J. Bao, Z. Lu, Y. Hong, Direct electrochemistry and electrocatalytic mechanism of evolved Escherichia coli cells in microbial fuel cells, Chem. Commun. (2008) 1290–1292.
[18] E. Mevers, L. Su, G. Pishchany, M. Baruch, J. Cornejo, E. Hobert, E. Dimise, C. M. Ajo-Franklin, J. Clardy, An elusive electron shuttle from a facultative anaerobe, eLife 8 (2019), https://doi.org/10.7554/elife.48054.
[19] J.R. Widhalm, C. Oostende, F. Furt, G.J.C. Basset, A dedicated thioesterase of the hotdog-fold family is required for the biosynthesis of the naphthoquinone ring of vitamin K 1, Proc. Natl. Acad. Sci. USA 106 (2009) 5599–5603, https://doi.org/10.1073/pnas.0900738106.
[20] L.T. Wey, P. Bombelli, X. Chen, J.M. Lawrence, C.M. Rabideau, S.J.L. Rowden, J. Z. Zhang, C.J. Howe, The development of biophotovoltaic systems for power generation and biological analysis, ChemElectroChem 6 (2019) 5375–5386, https://doi.org/10.1002/celc.201900997.
[21] M. Brachi, W. El Housseini, K. Beaver, R. Jadhav, A. Dantanarayana, D.G. Boucher, S.D. Minteer, Advanced electroanalysis for electrosynthesis, ACS Org. Inorg. Au 4 (2024) 141–187, https://doi.org/10.1021/acsorginorgau.3c00051.
[22] G. Bedendi, L.D. De Moura Torquato, S. Webb, C. Cadoux, A. Kulkarni, S. Sahin, P. Maroni, R.D. Milton, M. Grattieri, Enzymatic and microbial electrochemistry: approaches and methods, ACS Meas. Sci. Au 2 (2022) 517–541, https://doi.org/10.1021/acsmeasuresciau.2c00042.
[23] F. Crespi, Differential pulse voltammetry: evolution of an in vivo methodology and new chemical entries, a short review, JNDC 2 (2020) 20–28, https://doi.org/10.14302/issn.2377-2549.jndc-20-3298.
[24] H. Beitollahi, S. Zia Mohammadi, M. Safaei, S. Tajik, Applications of electrochemical sensors and biosensors based on modified screen-printed electrodes: a review, Anal. Methods 12 (2020) 1547–1560, https://doi.org/10.1039/C9AY02598G.
[25] J. Lopez-Tellez, S. Ramirez-Montes, T.A. Ferreira, E.M. Santos, J.A. Rodriguez, Application of voltammetric sensors for pathogen bacteria detection: a review, Chemosensors 10 (2022) 424, https://doi.org/10.3390/chemosensors10100424.
[26] M. Tucci, M. Grattieri, A. Schievano, P. Cristiani, S.D. Minteer, Microbial amperometric biosensor for online herbicide detection: photocurrent inhibition of *Anabaena variabilis*, Electrochim. Acta 302 (2019) 102–108, https://doi.org/10.1016/j.electacta.2019.02.007.
[27] R. Rippka, J. Deruelles, J.B. Waterbury, Generic assignments, strain histories and properties of pure cultures of cyanobacteria, J. Gen. Microbiol. 111 (1979) 1–61.
[28] R.J. Porra, W.A. Thompson, P.E. Kriedemann, Determination of accurate extinction coefficients and simultaneous equations for assaying chlorophylls *a* and *b* extracted with four different solvents: verification of the concentration of chlorophyll standards by atomic absorption spectroscopy, Biochimica et Biophysica Acta (BBA)-Bioenergetics 975 (1989) 384–394, https://doi.org/10.1016/S0005-2728(89)80347-0.
[29] Z. Rhodes, O. Simoska, A. Dantanarayana, K.J. Stevenson, S.D. Minteer, Using structure-function relationships to understand the mechanism of phenazine-mediated extracellular electron transfer in *Escherichia coli*, iScience 24 (2021), https://doi.org/10.1016/j.isci.2021.103033.
[30] G.G. Wildgoose, P. Abiman, R.G. Compton, Characterising chemical functionality on carbon surfaces, J. Mater. Chem. 19 (2009) 4875–4886, https://doi.org/10.1039/B821027F.
[31] M. Lu, R.G. Compton, Voltammetric pH sensing using carbon electrodes: glassy carbon behaves similarly to EPPG, Analyst 139 (2014) 4599–4605, https://doi.org/10.1039/C4AN00866A.
[32] X. Zhu, M.D. Yates, B.E. Logan, Set potential regulation reveals additional oxidation peaks of *Geobacter sulfurreducens* anodic biofilms, Electrochem. Commun. 22 (2012) 116–119, https://doi.org/10.1016/j.elecom.2012.06.013.
[33] L. Peng, X.-T. Zhang, J. Yin, S.-Y. Xu, Y. Zhang, D.-T. Xie, Z.-L. Li, *Geobacter sulfurreducens* adapts to low electrode potential for extracellular electron transfer, Electrochim. Acta 191 (2016) 743–749, https://doi.org/10.1016/j.electacta.2016.01.033.
[34] R.M. Egan, A.J. Victoria, J.Z. Zhang, Living photoanodes for solar-driven water oxidation, Chem. Rev. 126 (2026) 3529–3550, https://doi.org/10.1021/acs.chemrev.5c00921.